Structural transitions in the superconducting oxides Ba-Pb-Bi-O

Y. Koyama
Department of Materials Science and Engineering, Waseda University, 3-4-1 Ohkubo, Shinjuku-ku, Tokyo 169, Japan

M. Ishimaru*
Department of Metallurgy, Tokyo Institute of Technology, Oh-okayama, Meguro-ku, Tokyo 152, Japan
(Received 17 July 1991)

The crystal structures at room temperature and the structural transitions in $BaPb_{1-x}Bi_xO_3$ (Ba-Pb-Bi-O) have been investigated in detail by means of electron diffraction. From an analysis of the crystal structures on the basis of electron diffraction patterns obtained experimentally, it is shown that, as the temperature is lowered, Ba-Pb-Bi-O undergoes a cubic-to-tetragonal transition resulting from the condensation of the triply degenerate R_{25} mode, R^x_{25}, in the lower-Bi-content range $0 \le x < 0.35$, and successive transitions from the cubic to the tetragonal and to a monoclinic structure in the intermediate-Bi-content range $0.35 < x < 0.90$. In the successive transitions, the cubic-to-tetragonal transition is understood to be due to the first condensation of the R_{25} mode, R^x_{25}, and the tetragonal-to-monoclinic transition is due to the second condensation of the R_{25} mode, R^y_{25}. The soft-phonon-mode behavior of the R_{25} mode in the cubic and tetragonal phases was actually detected as a change in an intensity of diffuse scattering appearing at the R point in the first Brillouin zone of the cubic perovskite structure. In addition, the crystal structure at room temperature in the higher-Bi-content range $0.90 < x \le 1.00$ is confirmed to involve the breathing displacements resulting from the appearance of charge-density waves as well as the $R^x_{25} + R^y_{25}$ displacements. Moreover, a simple explanation of the physical origin of the superconductivity in Ba-Pb-Bi-O is presented on the basis of the present experimental results.

I. INTRODUCTION

$BaPb_{1-x}Bi_xO_3$ (Ba-Pb-Bi-O) is known to exhibit superconductivity.[1-6] It has been reported that superconductivity appears in the composition range $0 < x < 0.35$, and the highest T_c of about 12 K is obtained around $x = 0.25$. According to the band-structure calculation of Mattheiss and Hamann,[5] a hybridized orbital between 6*s*(Bi, Pb) and 2*P*(O) is understood to be responsible for superconductivity in Ba-Pb-Bi-O.

A basic crystal structure of Ba-Pb-Bi-O is the simple perovskite structure. Cox and Sleight[2,3] examined the crystal structures by means of neutron powder diffraction and showed that with increasing Bi content x, the crystal system undergoes the following changes: from an orthorhombic phase in the composition range $0 \le x < 0.05$, to a tetragonal one in $0.05 < x < 0.35$, to an orthorhombic one in $0.35 < x < 0.90$, and to a monoclinic one in $0.90 < x \le 1.00$. From the structures determined, the structures are understood to be related to the rotation (tilt) of oxygen octahedra in the perovskite structure. In addition, the breathing displacements of the oxygen atoms, which are due to the appearance of charge-density waves (CDW's) predicted from the band-structure calculation,[5] were found to be involved in the monoclinic system of $0.90 < x \le 1.00$.

In spite of the detailed analysis of the above-mentioned crystal structures, the space group of the orthorhombic system in $0.35 < x < 0.90$ has not been determined and features of structural transitions resulting in these structures are not understood at all. Because superconductivity in Ba-Pb-Bi-O appears in the tetragonal phase with $0 < x < 0.35$, understanding of the transitions is definitely necessary in order to elucidate the mechanism of the superconductivity. Thus motivated, we have examined the details of both the crystal structures at room temperature and the structural transitions with changing temperature in Ba-Pb-Bi-O by means of electron diffraction.

In the present paper, we report the crystal structures at room temperature in Ba-Pb-Bi-O, determined on the basis of the analysis of electron-diffraction patterns. In addition to the structures at room temperature, we describe features of the structural transitions, which were obtained by analyzing diffraction patterns taken at various temperatures in the low- and high-temperature stages of electron microscopy. In particular, we identify phonon modes responsible for the transitions in Ba-Pb-Bi-O. Furthermore, we briefly discuss a relation between the structural transitions and superconductivity on the basis of the present experimental results.

II. EXPERIMENTAL PROCEDURES

Powder samples of Ba-Pb-Bi-O with various x values were prepared from initial powders of $BaCO_3$, PbO, and Bi_2O_3 by means of a coprecipitation technique using citric acid. In order to avoid the evaporation of Pb, the powders were calcined in three steps: first at 773 K for 24 h, then at 873 K for 24 h, and finally at 973 K for 24 h. The powders were then pressed into pellets, followed by sintering at 1073 K for 24 h in air. Flakes of single crystals, obtained by crushing the pellets, were provided as a specimen for electron microscopy observation. The observation was made in the temperature range between

about 100 and 700 K by using a JEM-200CX electron microscope equipped with low- and high-temperature stages. In order to check the local composition of a specimen, an H-800 type electron microscope with energy-dispersive x-ray (EDX) spectroscopy was also used in the present experiment. Further, intensities of diffraction and diffuse spots in electron-diffraction patterns were measured by means of photodensitometry in order to examine the details of both the crystal structures and structural transitions.

III. EXPERIMENTAL RESULTS

A. Crystal structures at room temperature

The features of electron-diffraction patterns are basically the same for Ba-Pb-Bi-O with different x. As an example, electron-diffraction patterns of Ba-Pb-Bi-O with $x=0.25$, taken at room temperature, are shown in Fig. 1. The electron incidences of Figs. 1(a), 1(b), and 1(c) are, respectively, parallel to the $[1\bar{1}0]$, $[00\bar{1}]$, and $[1\bar{1}\,\bar{1}]$ directions.

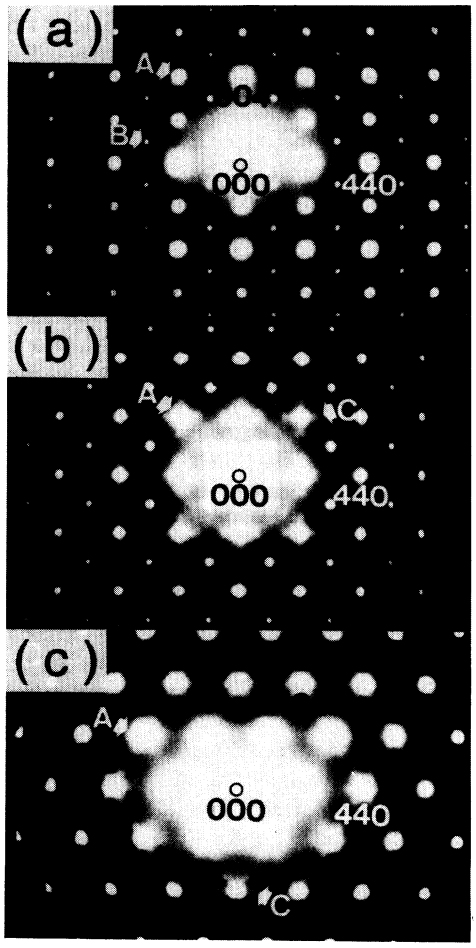

FIG. 1. Electron-diffraction patterns of Ba-Pb-Bi-O with $x=0.25$ taken at room temperature. Electron incidences for (a), (b), and (c) are, respectively, parallel to the $[1\bar{1}0]$, $[00\bar{1}]$, and $[1\bar{1}\,\bar{1}]$ directions.

tions. In the patterns there exist three types of scatterings, indicated by A, B, and C. Scattering types A and C have the same features for all x, but the details of scattering type B are x dependent. From the analysis of the diffraction patterns, spots with strong intensity, due to scattering type A, are understood to be fundamental spots of Ba-Pb-Bi-O. Because the fundamental spots have an extinction rule of h,k, and $1=2n+1$ (n integer) in terms of a $2a_0\times 2a_0\times 2a_0$ supercell, the spots are due to a simple perovskite structure as the basic structure, where a_0 is the lattice parameter of the pseudocubic structure. Scattering type C is diffuse scattering around the fundamental spot, which is elongated along $\langle 110\rangle$ directions. Note that this diffuse scattering has previously been found by other investigators.[7,8] As they have pointed out, its physical origin is understood to be mainly due to atomic displacements of metal atoms, which are produced by the existence of oxygen vacancies. Because scattering types A and C are not directly related to structural transitions, the most important feature in the diffraction patterns of Ba-Pb-Bi-O is scattering type B, which is presumably due to oxygen-atom displacements in the transitions, as will be described below.

Scattering type B is characterized by a diffraction spot with weaker intensity and is identified as a superlattice spot showing a superstructure in the perovskite structure. A careful analysis of the diffraction patterns shows that the superlattice spots are located at the zone boundary of the first Brillouin zone of the cubic perovskite structure along $\langle 111\rangle$ directions, that is, the R point. This suggests that atomic displacements related to the superlattice spots result from the condensation of phonon modes at the R point. Hence possible displacements in Ba-Pb-Bi-O should be due to the condensation of the R_{25} mode[9] or the breathing mode,[5] but are never related to the M_3 mode,[10] which is a phonon mode at the zone boundary along $\langle 110\rangle$ directions.

The intensity analysis of the superlattice spots at the R point indicates that the crystal structures are associated with three composition ranges: (i) $0\le x<0.35$, (ii) $0.35<x<0.90$, and (iii) $0.90<x\le 1.00$. Note that superlattice spots in diffraction patterns are indexed in terms of the $2a_0\times 2a_0\times 2a_0$ supercell, just as in the case of the fundamental spots. Figure 2, first of all, shows three electron-diffraction patterns for $x=0.25$, which belong to the lower-Bi-content group (a). The pattern of Fig. 2(a) was taken with an electron incidence parallel to the $[1\bar{1}0]$ direction. In order to avoid double diffraction, the specimen is rotated about the [111] and $[11\bar{1}]$ directions. The patterns of Figs. 2(b) and 2(c) were then taken in the cases of the rotations about the [111] and $[11\bar{1}]$ directions, respectively. As can be seen in Fig. 2, spots with $|h|=|k|=|l|=2n+1$ are missing. From other diffraction patterns as well as those in Fig. 2, the extinction rule for $x=0.25$ is confirmed to be $|h|=|k|=|l|=2n+1$ in terms of the supercell. The most important thing is that this rule is identical to that obtained from three variants, in each of which the R_{25} displacements along one axis take place. Note that the R_{25} mode is one of the rotation (tilt) modes of the oxygen octahedra in the perovskite structure. In the present paper, the ro-

tation axis in each variant is, for convenience's sake, assumed to be the x axis. Then the condensation mode is written as the R_{25}^{x} mode.

In order to confirm the above result, the intensities of the superlattice spots were measured by means of photodensitometry and compared with those calculated from the R_{25}^{x} displacements. The intensity was experimentally determined in the following way. A series of electron-diffraction patterns were first taken by rotating a specimen in an angle step of about 0.17°, and the intensities of the superlattice spots in each pattern were measured by photodensitometry. Then the intensity-vs-azimuth curve for each superlattice spot was drawn and the strongest intensity in the curve was adopted as a measured intensity. Figure 3 shows a comparison between the measured intensities determined by this procedure and the calculated intensities obtained from the R_{25}^{x} displacements for some superlattice spots. Because of the long extinction distance for the superlattice spot, the calculation was made in terms of kinematical theory. In the calculation three variants were taken into account and the magnitude of

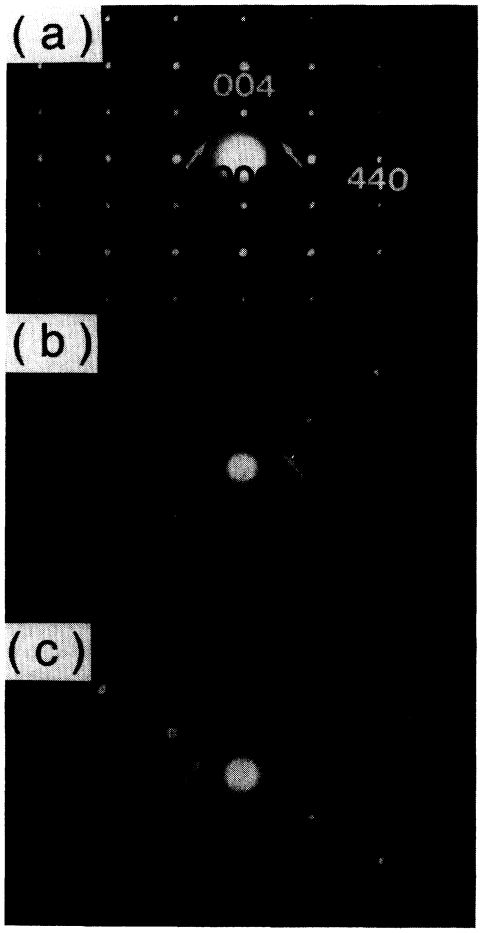

FIG. 2. Electron-diffraction patterns of Ba-Pb-Bi-O with $x=0.25$. The electron incidence for (a) is parallel to the $[1\bar{1}0]$ direction. The patterns of (b) and (c) were taken by rotating the specimen about the [111] and $[11\bar{1}]$ directions, respectively. The 111 and $\bar{1}\,\bar{1}1$ superlattice spots indicated by the arrows in (a) vanish in (b) and (c).

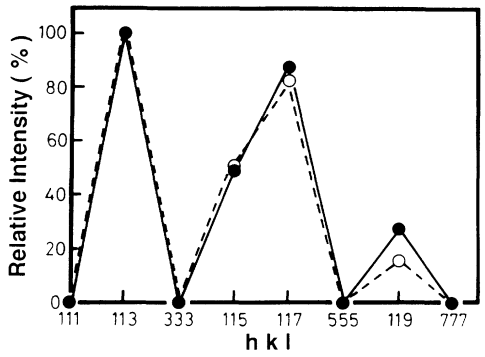

FIG. 3. Comparison between experimentally obtained intensities, indicated by solid circles and calculated ones by open circles, for some superlattice spots in the case of $x=0.25$. The intensities are normalized with respect to the intensity of the 113 superlattice spot.

the displacement of the oxygen atom for the rotation was assumed to be $\bar{x}=0.27$ Å on the basis of Landau theory, which will be described later. From Fig. 3 it is easy to understand that the measured intensities are in very good agreement with the calculated ones. Hence the atomic displacements in $0\leq x<0.35$ are concluded to be those expected from the condensation of the triply degenerate R_{25} mode along one axis. As a result of the condensation, the crystal system in Ba-Pb-Bi-O with $0\leq x<0.35$ is the tetragonal system whose space group is $I4/mcm$ and the lattice parameters were determined to be $a=6.065$ Å and $c=8.587$ Å for $x=0.25$ from x-ray powder diffraction. Furthermore, in the present experiment, the crystal structure in $0\leq x<0.05$ was not found to be different from that in $0.05<x<0.35$, although Cox and Sleight[2,3] reported that the crystal systems are, respectively, the orthorhombic system in the former and the tetragonal one in the latter. Based on our results, it should be said that Ba-Pb-Bi-O with $0\leq x<0.05$ also has the tetragonal system (space group $I4/mcm$).

The same experiment as that performed in the lower-Bi-content range (i) was made in order to examine the crystal structure of samples in the intermediate-Bi-content range (ii). Electron-diffraction patterns of Ba-Pb-Bi-O with $x=0.50$ are, for instance, shown in Fig. 4. The superlattice spots with $|h|=|k|=|l|=2n+1$ are seen in the patterns. That is, there is no extinction rule for the superlattice spots at the R point in this case. Then, in order to determine the crystal structure, the intensities of the superlattice spots were measured in the same procedure as that in $0\leq x<0.35$ and are shown in Fig. 5. Intensities calculated based on the $R_{25}^{x}+R_{25}^{y}$ displacements are also plotted. In the calculation the magnitudes of the displacements for the rotations about the x and y axes are, respectively, assumed to be $\bar{x}=0.30$ Å and $\bar{y}=0.23$ Å, which are obtained theoretically on the basis of Landau theory. Although only a single variant is taken into account in the calculation, the intensities obtained from multiple variants are almost equal to those from the single variant. That is, the adoption of multiple variants in the calculation never changes the essential features shown in Fig. 5. As is easily seen in Fig. 5, the

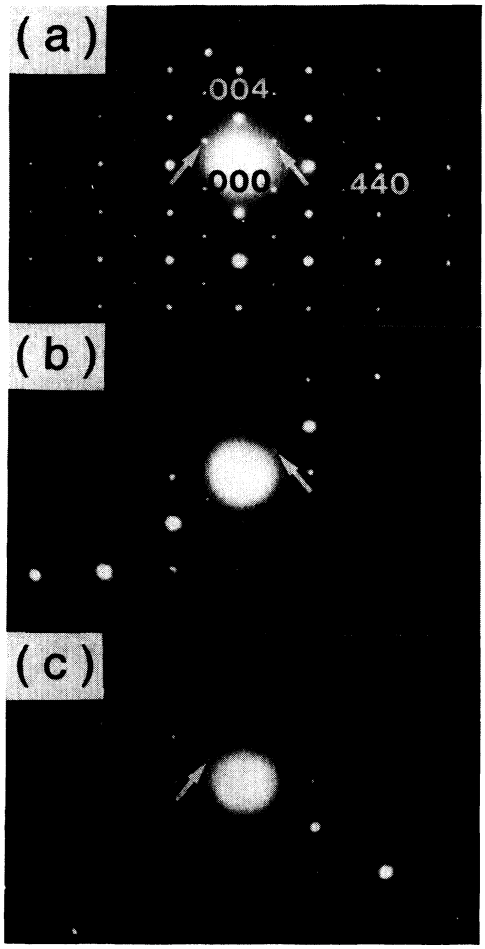

FIG. 4. Electron-diffraction patterns of Ba-Pb-Bi-O with $x=0.50$ taken at room temperature. The condition for taking the patterns of (a), (b), and (c) are the same as in the case of $x=0.25$. The 111 and $\bar{1}\bar{1}1$ spots indicated by the arrows are found in (a), (b), and (c).

agreement between the measured and calculated intensities is excellent. Hence, not only the R_{25}^{x} displacements observed in $0\leq x<0.35$, but also the R_{25}^{y} ones are understood to take place in $0.35<x<0.90$, where the axis of the second rotation is assumed to be the y axis. According to Glazer,[11] the $R_{25}^{x}+R_{25}^{y}$ displacements with the different magnitudes result in the monoclinic system whose space group is $I2/m$. Unfortunately, it is impossible to determine lattice parameters precisely in the monoclinic system because of experimental errors, and so they are not specified here. In any case, this result is quite different from the conclusion that the system is orthorhombic as previously reported by Cox and Sleight.[3] Further, because the magnitude of the displacement for the R_{25}^{x} displacements is not equal to that for the R_{25}^{y} ones, the rotation axis of the oxygen octahedra obviously deviated from the [110] direction.

In addition to the $R_{25}^{x}+R_{25}^{y}$ displacements, the breathing displacements of the oxygen atoms are involved in the crystal structure for the higher-Bi-content range (iii). The $R_{25}^{x}+R_{25}^{y}+$ breathing displacements produce no extinction rule for the superlattice spots at the R point in terms of the supercell, just as in the intermediate-Bi-content range $0.35<x<0.90$. Actually, all spots are observed in electron-diffraction patterns of Fig. 6. In order to confirm the condensation of the breathing mode, the intensities of the superlattice spots were determined in

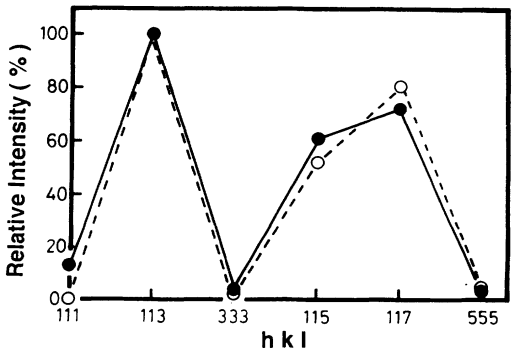

FIG. 5. Comparison between experimentally obtained intensities (solid circles) and calculated ones (open circles) for some superlattice spots in the case of $x=0.50$. The intensities are normalized with respect to the intensity of the 113 spot.

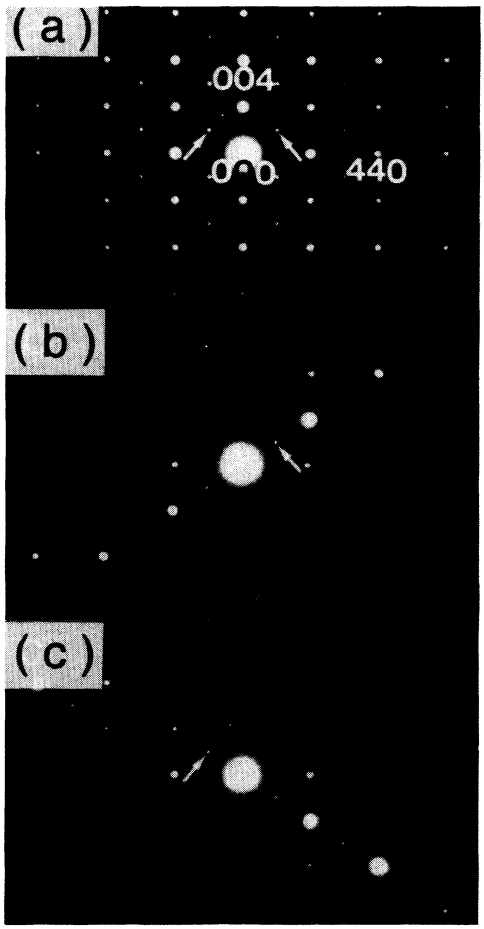

FIG. 6. Electron-diffraction patterns of Ba-Pb-Bi-O with $x=1.00$ taken at room temperature. The condition for taking the patterns of (a), (b), and (c) are the same as in $x=0.25$ and 0.50. The 111 and $\bar{1}\bar{1}1$ spots indicated by arrows appear in (a), (b), and (c), just as in $x=0.50$.

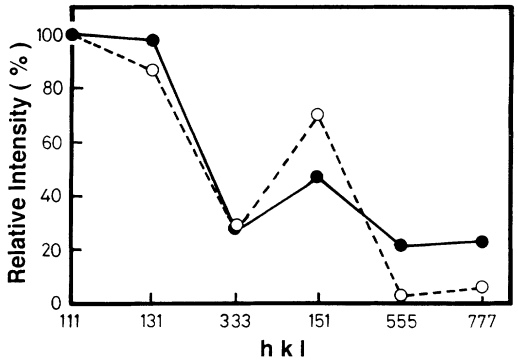

FIG. 7. Comparison between experimentally obtained intensities (solid circles) and calculated ones (open circles) for some superlattice spots in the case of $x=1.00$. The intensities are normalized with respect to the intensity of the 111 spot.

the same way as in the lower- and intermediate-Bi-content ranges $0 \leq x < 0.35$ and $0.35 < x < 0.90$. Theoretical intensities were calculated, taking multiple variants into account, in the assumption that $\bar{x}=\bar{y}=0.28$ Å and the breathing displacements of 0.08 Å. These magnitudes are those reported by Cox and Sleight.[2] In Fig. 7 the measured intensities of the spots are shown to be in good agreement with the calculated ones for the $R_{25}^{x}+R_{25}^{y}+$ breathing displacements, and the crystal system is then monoclinic. Note that in order to distinguish the two monoclinic systems in Ba-Pb-Bi-O the systems in $0.35 < x < 0.90$ and $0.90 < x \leq 1.00$ are, respectively, called the monoclinic(I) and monoclinic(II) systems. Further, the agreement between the measured and calculated intensities clearly implies that the condensation of the breathing mode as well as the $R_{25}^{x}+R_{25}^{y}$ mode occurs in Ba-Pb-Bi-O with $0.90 < x \leq 1.00$. In other words, the CDW exists in a three-dimensional system, as pointed out in previous works.[2,3] Although the CDW in a three-dimensional system has been reported in the case that the Coulomb field due to the CDW is screened mainly by means of the introduction of antiphase boundaries,[12,13] Ba-Pb-Bi-O is the first case where only the atomic displacements screen the field. Eventually, Ba-Pb-Bi-O with $0.90 < x \leq 1.00$ is confirmed to have the monoclinic(II) system (space group $P2/m$), which was reported by Cox and Sleight.[2,3]

B. Structural transitions in Ba-Pb-Bi-O

From an examination of the crystal structures at room temperature, structural transitions due to the R_{25} mode should take place in Ba-Pb-Bi-O. In order to understand the features of the transitions, low- and high-temperature experiments have been carried out. In the case of $0 \leq x < 0.35$, the R_{25}^{x} displacements are involved in the crystal structure on the basis of the analysis of the electron-diffraction patterns. Hence the cubic-to-tetragonal transition related to the condensation of the R_{25}^{x} mode should be expected to occur at a higher-temperature. Figure 8 shows electron-diffraction patterns of Ba-Pb-Bi-O with $x=0.25$, taken in the process of heating and subsequent cooling. In the pattern at room temperature [Fig. 8(a)], there exist strong superlattice spots indicating the existence of the R_{25} displacements. When the temperature is raised, intensities of the superlattice spots become weaker [Fig. 8(b)], and then the spots disappear around 540 K [Fig. 8(c)]. This implies that the cubic-to-tetragonal transition takes place around 540 K. When the specimen is then cooled to room temperature, the superlattice spots are again observed in the pattern, as shown in Fig. 8(d). Hence the change in the intensity of the spot is reversible during the heating and

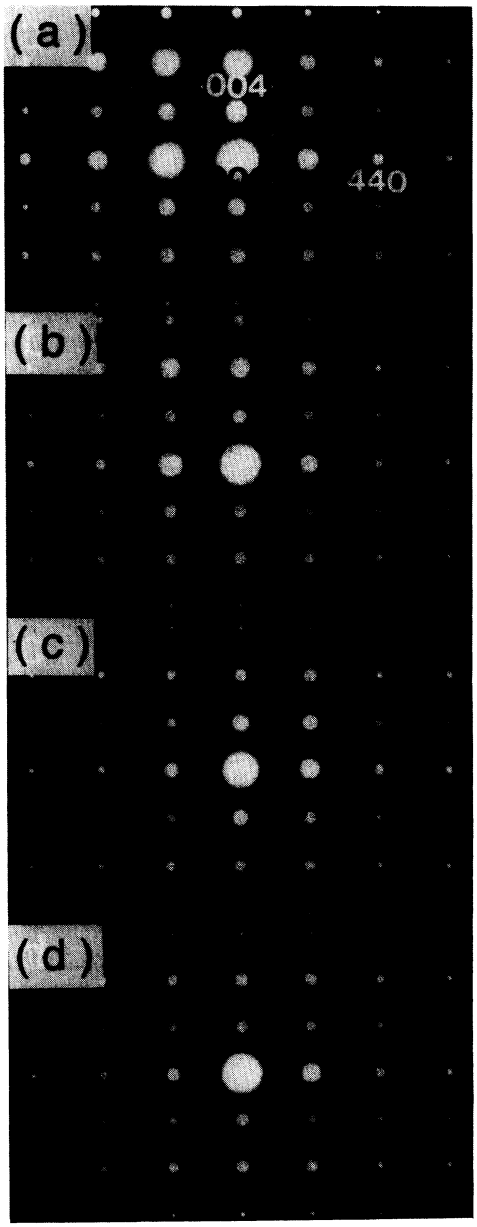

FIG. 8. Electron-diffraction patterns of Ba-Pb-Bi-O with $x=0.25$ at various temperatures during the process of heating and subsequent cooling. Electron incidences for all patterns are parallel to the $[1\bar{1}0]$ direction. The patterns were, respectively, taken at (a) room temperature, (b) 450 K, (c) 540 K, and (d) room temperature.

cooling cycles. Figure 9 shows the temperature dependence of a measured intensity of the 311 superlattice spot in $x=0.25$. The intensity at each temperature was measured from the obtained diffraction pattern by means of photodensitometry. In the figure the solid line represents intensities calculated from displacements obtained on the basis of Landau theory[9] for the transition due to the condensation of the R_{25} mode. As the temperature increases, the intensity decreases and reaches zero around 540 K. The most important thing is that when the parameters in Eq. (8) of Ref. 9 are assumed to be $T_0=540$ K and $(a/4A')^{1/2}=0.002$, the theory reproduces well the change obtained experimentally. In other words, it can be theoretically confirmed that the structural transition is due to the condensation of the R_{25} mode. In addition to Ba-Pb-Bi-O with nonzero x, $BaPbO_3$ ($x=0$) was also found to exhibit a cubic-to-tetragonal transition around 480 K. Accordingly, the R_{25}^x displacements obtained from the analysis of the diffraction patterns at room temperature are actually understood to result from the condensation of the R_{25}^x mode, just as in $SrTiO_3$.

A phonon mode with low frequency can be detected as thermal diffuse scattering in electron diffraction. Hence the softening of the R_{25} mode in the cubic phase has been examined as a change in an intensity of diffuse scattering for $x=0.25$. An electron-diffraction pattern at 543 K for $x=0.25$ is shown in Fig. 10. In the pattern diffuse scattering, indicated by an arrow, is clearly observed at the zone boundary of the first Brillouin zone along the $\langle 111 \rangle$ directions: the R point. When the temperature is lowered, the diffuse scattering becomes a superlattice spot due to the R_{25}^x displacements at a transition temperature of about 540 K. In addition, the change in the intensity of the diffuse scattering is reversible during the cooling and heating cycles. Because of these, the diffuse scattering is easily understood to be related to the soft R_{25} mode. Figure 11 shows the temperature dependence of the diffuse scattering intensity measured from diffraction patterns taken at three temperatures of the cubic phase. From Fig. 11, when the temperature is lowered toward a

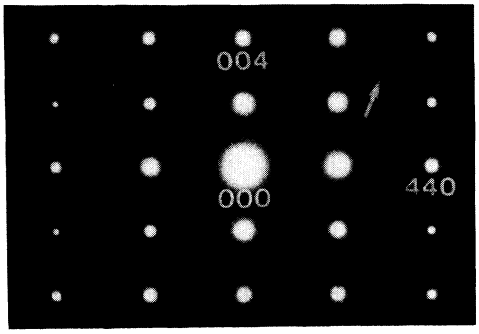

FIG. 10. Electron-diffraction pattern taken at 543 K for $x=0.25$. The electron incidence is parallel to the $[1\bar{1}0]$ direction.

transition temperature of 540 K, the measured intensity increases remarkably. Because the intensity of the thermal diffuse scattering is inversely proportional to the square of the frequency of the phonon mode,[14] the increase in intensity basically indicates the softening of the R_{25} mode. Note that the diffuse scattering also involves the contribution of the quasielastic scattering accompanied by the softening where the scattering is observed as a central peak in neutron diffraction. Unfortunately, the separation of the quasielastic scattering from the total scattering cannot be made in electron diffraction. Anyway, the increase in the intensity is direct evidence that the transition originates from the soft phonon mode of the triply degenerate R_{25} mode.

The successive transitions from cubic to tetragonal and then to monoclinic(I) would take place in $0.35<x<0.90$. From the analysis of the crystal structure at room temperature, it seems that the transition from cubic to tetragonal occurs as a result of the condensation of the R_{25}^x mode, just as in the case of $0\leq x<0.35$, and the tetragonal-to-monoclinic(I) transition is due to the condensation of the R_{25}^y mode. From this motivation a change in diffraction patterns with changing temperature has been examined for $x=0.50$, as shown in Fig. 12.

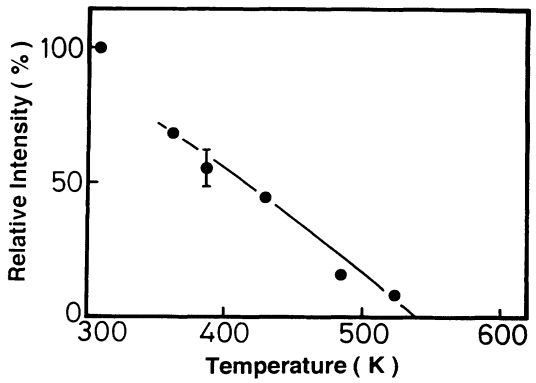

FIG. 9. Temperature dependence of the intensity of the 311 superlattice spot for $x=0.025$. The solid curve is calculated by using the magnitude of the displacement, which is obtained on the basis of Landau theory for the cubic-to-tetragonal transition in $SrTiO_3$.

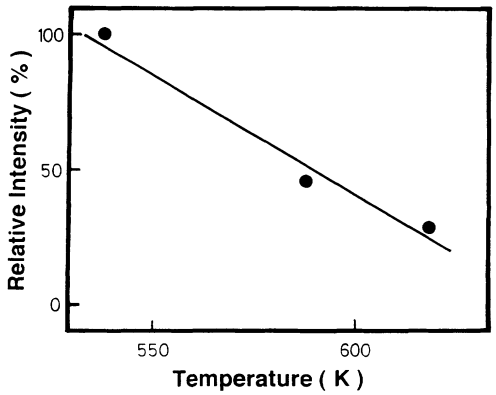

FIG. 11. Temperature dependence of the intensity of thermal diffuse scattering observed at the R point of the cubic phase for $x=0.25$. The intensities are normalized with respect to the intensity at 543 K.

When the temperature is raised, superlattice spots with strong intensity at the R point [Figs. 12(a) and 12(b)] become weaker, and then the spots with $|h|=|k|=|l|=2n+1$ first vanish around 470 K [Figs. 12(c) and 12(d)]. The disappearance of these spots clearly implies that Ba-Pb-Bi-O with $x=0.50$ exhibits the monoclinic(I)-to-tetragonal transition on heating. On further heating all superlattice spots disappear in the diffraction patterns around 600 K [Fig. 12(e)]. That is, this corresponds to the tetragonal-to-cubic transition. The same experiments were made for Ba-Pb-Bi-O with different x in $0.35<x<0.90$, and the existence of the successive transition was confirmed. Eventually, when the temperature is lowered from the cubic phase, Ba-Pb-Bi-O with $0.35<x<0.90$ exhibits a cubic-to-tetragonal transition at a higher temperature and a tetragonal-to-monoclinic(I) transition at a lower temperature. It is obvious that the former transition results from the first condensation of the triply degenerate R_{25} mode R^{x}_{25} and the latter is due to the second condensation R^{y}_{25}.

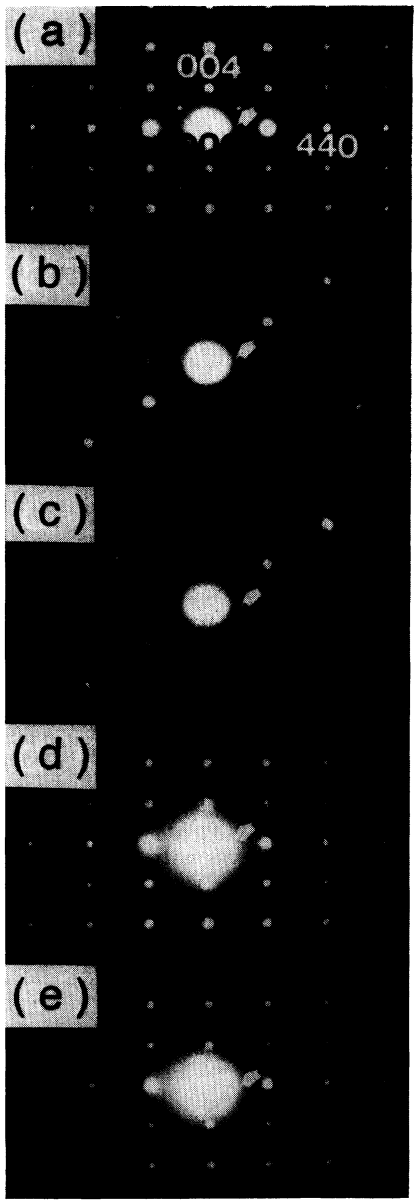

FIG. 12. Electron-diffraction patterns of Ba-Pb-Bi-O with $x=0.50$ at various temperatures during the heating process. The pattern were taken at room temperature for (a) and (b), at 470 K for (c) and (d), and at 600 K for (e). Electron incidences for (a), (d), and (e) are parallel to the $[1\bar{1}0]$ direction, although the patterns for (b) and (c) were taken by rotating the specimen about the [111] direction in order to obtain the double-diffraction free condition. Because the 111 superlattice spot indicated by the arrow vanishes in (c), the spot observed in (d) is due to the double diffraction.

As the softening of the R_{25} mode in the cubic-to-tetragonal transition was already reported, we show the softening of the R^{y}_{25} mode in the tetragonal-to-monoclinic(I) transition here. Figure 13 shows electron-diffraction patterns taken at 297, 393, and 468 K in the tetragonal phase for $x=0.40$. Note that the tetragonal-to-monoclinic(I) transition in $x=0.40$ takes place around 280 K, which is just below room temperature. It is found that at 297 K diffuse scattering exists at positions where the superlattice spots with $|h|=|k|=|l|=2n+1$ appear in the monoclinic(I) phase. Hence the diffuse scattering at these positions is identified as diffuse scattering related to the soft R^{y}_{25} mode. Further, intensities of the diffuse scattering indicated by arrows are found to de-

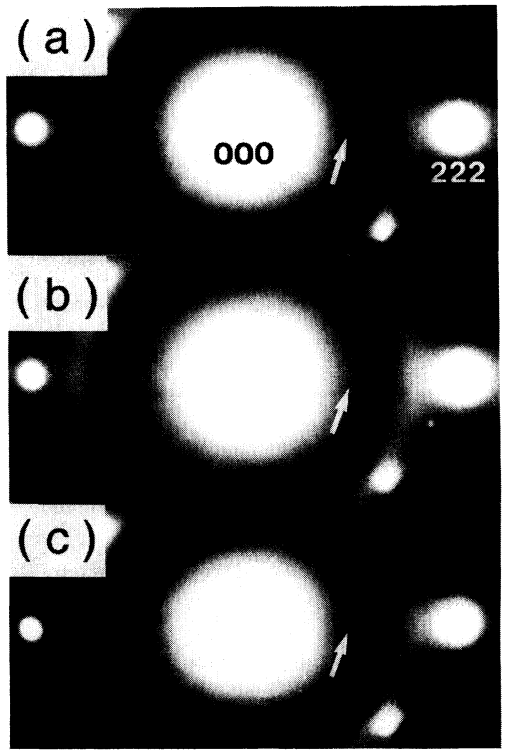

FIG. 13. Electron-diffraction patterns showing a change in the intensity of thermal diffuse scattering in the tetragonal phase taken at (a) 297 K, (b) 393 K, and (c) 468 K, respectively. The specimen is slightly rotated in order to avoid the double diffraction. A halo pattern observed is due to a carbon film used for coating a copper grid.

crease with increasing temperature. The intensity at 468 K is actually very weak. The temperature dependence of the intensity measured from diffraction patterns taken at various temperatures in the tetragonal phase is shown in Fig. 14. When the temperature is lowered toward the transition temperature of the tetragonal-to-monoclinic(I) transition, the intensity of the diffuse scattering is shown to increase in the figure. In particular, a remarkable change is observed around room temperature, that is, just above the transition temperature. Accordingly, this change is direct evidence that the R_{25}^{y} mode exhibits soft-mode behavior in the tetragonal-to-monoclinic(I) transition. In other words, the R_{25}^{y} mode is concluded to be very soft in the tetragonal phase.

In electron microscopy observation, a specimen is placed in vacuum of about 10^{-7} Torr. The evaporation of the oxygen atoms, which leads to the formation of oxygen vacancies, would easily occur, particularly in $BaBiO_3$, when the specimen is heated. Actually, diffraction patterns of $BaBiO_3$, taken at a higher temperature, exhibit superlattice spots at the $\frac{1}{6}$ positions between two neighboring fundamental spots along $\langle 110 \rangle$ directions, as seen in Fig. 15. Because these spots are also produced by electron-beam irradiation, a modulated structure characterized by spots at the $\frac{1}{6}$ positions should be understood to be caused by the periodic arrangement of oxygen vacancies. In other words, unfortunately, we cannot examine the structural transition of $BaBiO_3$ above room temperature.

Moreover, electron-beam irradiation often produces superlattice spots at the $\frac{1}{2}$ or $\frac{1}{4}$ positions between two fundamental spots along $\langle 110 \rangle$ directions in the case of $x < 0.90$. As in the case of the spots at the $\frac{1}{6}$ positions in $BaBiO_3$, these spots are also due to the ordering of the oxygen vacancies induced by the irradiation. Note that, because they are directly related to the existence of the oxygen vacancies, these spots basically have the same physical origin as the scattering type C mentioned earlier. It should be further stressed that in the present experiment the transitions due to the R_{25} mode were found to be suppressed by the existence of the oxygen vacancies.

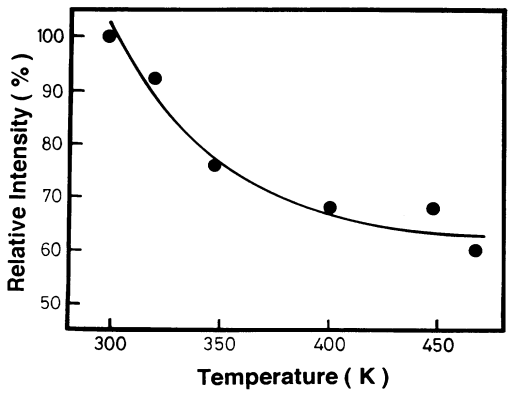

FIG. 14. Temperature dependence of the intensity of thermal diffuse scattering due to the soft R_{25}^{y} mode in the tetragonal phase. The intensities are normalized with respect to the intensity at 297 K.

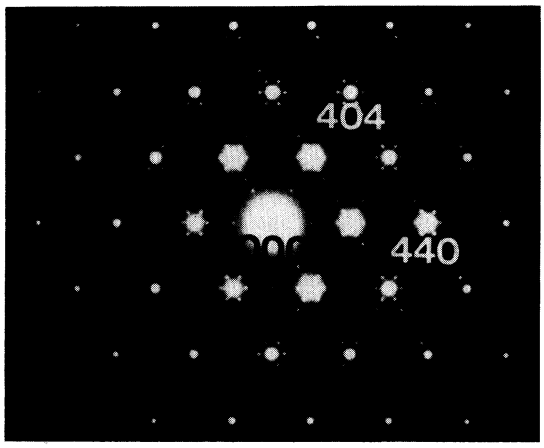

FIG. 15. Electron-diffraction pattern of Ba-Pb-Bi-O with $x = 1.00$ taken at about 400 K. The electron incidence is parallel to the $[1\bar{1}\,\bar{1}]$ direction.

In other words, these spots are not related to both the appearance of the CDW and the structural transitions due to the condensation of the R_{25} mode at all, although the existence of the CDW spots with an incommensurate period in diffraction patterns has been reported in $Ba_{1-y}K_yBiO_3$ (Ba-K-Bi-O).[15]

Pei *et al.*[16] found the appearance of new Bragg peaks in neutron powder patterns of $BaBiO_3$ below 150 K. This suggests that a phase transition should take place around 150 K. Based on their results, it is predicted that superlattice spots appear at the $\frac{1}{2}$ positions between two fundamental spots along $\langle 110 \rangle$ directions. In order to confirm this, we conducted a low-temperature experiment by means of the low-temperature stage with a liquid-nitrogen reservoir. Figure 16 is an electron-diffraction pattern of $BaBiO_3$ taken at about 110 K. The electron incidence is parallel to the $[00\bar{1}]$ direction. No superlattices spot can be found at the $\frac{1}{2}$ positions. Then it must be concluded that as the temperature is lowered from room temperature, $BaBiO_3$ does not undergo a phase transition, at least not above about 100 K.

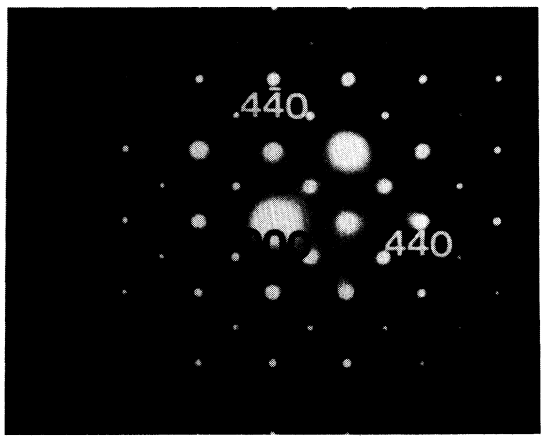

FIG. 16. Electron-diffraction pattern of Ba-Pb-Bi-O with $x = 1.00$ taken at about 110 K.

IV. DISCUSSION

The present experiment clearly shows that in Ba-Pb-Bi-O there exists structural transitions which can be ascribed to the condensation of the triply degenerate R_{25} mode. That is, the cubic-to-tetragonal transition due to the condensation of the R_{25}^{x} mode exists in $0 \leq x < 0.35$ and the successive transitions from cubic to tetragonal and further monoclinic(I) occur on cooling in $0.35 < x < 0.90$. Note that the cubic-to-tetragonal transition in the successive transitions is due to the first condensation of the R_{25} mode, R_{25}^{x}, and the tetragonal-to-monoclinic(I) one due to the second condensation R_{25}^{y}. Figure 17 is a phase diagram in the range of $0 \leq x < 0.8$, which is determined from the present data. From the phase diagram, with increasing Bi content x, the transition temperature of the cubic-to-tetragonal transition gradually increases from 480 K at $x = 0$ to about 600 K at $x = 0.8$, while in $0.4 < x < 0.8$ the increase in the transition temperature of the tetragonal-to-monoclinic(I) transition is more rapid. In addition, although a structural transition cannot be examined in $0.90 < x \leq 1.00$, the crystal structure at room temperature was confirmed to involve the breathing displacements as well as the R_{25} ones. The breathing displacements are understood to be directly related to the appearance of the CDW in a three-dimensional system on the basis of the calculation of the band structure.[5]

Successive transitions were found to take place in $0.35 < x < 0.90$ in the present work. As is understood from Fig. 17, the difference in the transition temperature between the cubic-to-tetragonal and tetragonal-to-monoclinic(I) transitions becomes smaller for larger x. Because of this fact, the magnitude of the displacement at room temperature for the rotation about the y axis is much smaller than that about the x axis around $x = 0.5$ and is almost equal to that around $x = 0.8$. In other words, around $x = 0.8$ the rotation axis of the oxygen octahedra deviates very little from the [110] direction and the intensities of the superlattice spots at the R point are approximately equal to those obtained from the condensation of the R_{25}^{x} and R_{25}^{y} modes at the same time, which leads to the orthorhombic system as a crystal system. This is the reason why the space group of the monoclinic system in $0.35 < x < 0.90$, which was thought to be the orthorhombic system before, has not been determined until the present work.

The structural transitions in Ba-Pb-Bi-O can be explained in terms of the Landau theory proposed for the cubic-to-tetragonal transition in $SrTiO_3$,[9] which is due to the condensation of the R_{25} mode. In Fig. 9 the temperature dependence of the intensity of the superlattice spot is actually reproduced by using $T_0 = 540$ K and $(a/4A')^{1/2} = 0.002$, which are parameters in the theory. In the analysis of the crystal structures at room temperature, the magnitude of the displacement in the calculation of the intensity was determined by assuming $(a/4A')^{1/2} = 0.002$ for $x = 0.25$ and 0.50. The transition temperatures obtained experimentally were also used as T_0 in the calculation. The value of T_0 for $x = 0.25$ is 540 K, while there are two T_0's for $x = 0.50$, which correspond to the successive transition. The magnitudes of $\bar{x}$ and $\bar{y}$ in $x = 0.50$ were, respectively, obtained from $T_0 = 600$ and 470 K in the present work. On the other hand, because the structural transition for $x = 1.00$ could not be examined, the intensities were calculated by the magnitudes of the R_{25} and breathing displacements, which were determined by Cox and Sleight.[2] Eventually, the intensities of the superlattice spots at room temperature for $x = 0.25$, 0.50, and 1.00, which were calculated by using the above parameters, can reproduce well the experimental intensities. This fact is taken to be further theoretical support for the interpretation that the transition in Ba-Pb-Bi-O is basically due to the condensation of the R_{25} mode.

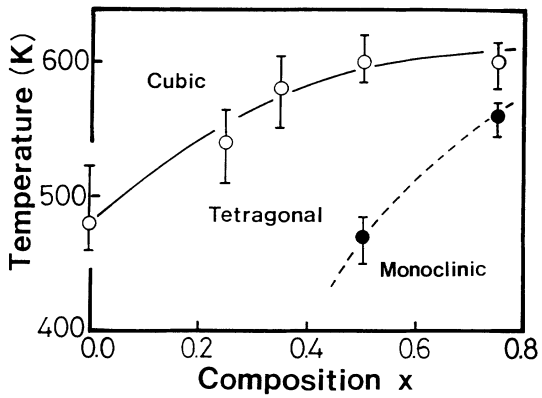

FIG. 17. Determined phase diagram of Ba-Pb-Bi-O in the region between $x = 0$ and 0.8 above 400 K. The solid curve denotes the transition temperature of the cubic-to-tetragonal transition, and the dashed curve represents the temperature of the tetragonal-to-monoclinic(I) transition.

Superlattice spots with the incommensurate period in diffraction patterns were found in Ba-K-Bi-O (Ref. 15) and thought to be due to CDW's, which are not related to the CDW resulting in the breathing displacements. In the present experiment, however, the superlattice spots, except for the spots at the R point, are understood to be induced by electron-beam irradiation. This clearly implies that the CDW's with an incommensurate period do not exist in Ba-Pb-Bi-O. Hence the present experiment never supports the mechanism of superconductivity, which is based on the CDW's with an incommensurate period.

Superconductivity in Ba-Pb-Bi-O has been explained in terms of the breathing mode due to the CDW. With this viewpoint, the relatively high-T_c results from a strong electron-phonon coupling produced from the instability for the CDW. Because of this, superconductivity with high T_c must be realized only in the monoclinic(I) phase near the boundary between the monoclinic(I) and monoclinic(II) phases. However, superconductivity is obtained in the tetragonal phase. From these facts we cannot believe that the breathing mode is mainly responsible for superconductivity in Ba-Pb-Bi-O.

On the basis of the present results, the mechanism of superconductivity is briefly discussed. In Landau theory[9] for the transition due to the R_{25} mode, the order parame-

ter is the triply degenerate set of the soft-mode coordinates. It is worth noting that the order parameter can be coupled to spontaneous strains corresponding to the A_{1g}, E_g, and T_{2g} irreducible representations of the point group O_h, as shown in the case of $SrTiO_3$.[9] This implies that the fluctuation of the order parameter in the cubic and tetragonal phases produces that of the spontaneous strains. In addition, the strains corresponding to the A_{1g} and E_g representations lead to a change in the Coulomb potential on the Bi (Pb) site. In other words, the electron-phonon coupling resulting from the fluctuation of these strains would play an important role in superconductivity. Hence it is possible to explain superconductivity in Ba-Pb-Bi-O in relation to the structural transition. The details of the correlation between the transition and superconductivity will be described elsewhere.

ACKNOWLEDGMENT

The authors would like to thank S. Nakamura for help in the high-temperature experiment.

*Present address: Department of Materials Science and Technology, Kyushu University, Kasuga, Fukuoka 816, Japan.

[1]A. W. Sleight, J. L. Gillson, and P. E. Bierstedt, Solid State Commun. **17**, 27 (1975).

[2]D. E. Cox and A. W. Sleight, Solid State Commun. **19**, 969 (1976).

[3]D. E. Cox and A. W. Sleight, in *Proceedings of the Conference on Neutron Scattering, Gatlinburg, Tennessee, 1976,* edited by R. M. Moon (National Technical Information Service, Springfield, VA, 1976), p. 45.

[4]T. M. Rice and L. Sneddon, Phys. Rev. Lett. **47**, 689 (1981).

[5]L. F. Mattheiss and D. R. Hamann, Phys. Rev. B **28**, 4227 (1983).

[6]S. Tajima, S. Uchida, A. Masaki, H. Takagi, K. Kitazawa, S. Tanaka, and S. Sugai, Phys. Rev. B **35**, 696 (1987).

[7]E. A. Hewat, C. Chaillout, M. Godinho, M. F. Gorius, and M. Marezio, Physica C **157**, 228 (1989).

[8]C. Chaillout and J. P. Remieka, Solid State Commun. **56**, 833 (1985).

[9]J. C. Slonczewski and H. Thomas, Phys. Rev. B **1**, 3599 (1970).

[10]S. Hirotsu, J. Harada, M. Iizumi, and K. Gesi, J. Phys. Soc. Jpn. **37**, 1393 (1974).

[11]A. M. Glazer, Acta Crystallogr. B **28**, 3384 (1972).

[12]Y. Koyama, J. Yoshida, H. Hoshiya, and Y. Nakamura, Phys. Rev. B **40**, 5378 (1989).

[13]Y. Koyama and M. Ishimaru, Phys. Rev. B **41**, 8522 (1990).

[14]M. Born and K. Sarginson, Proc. R. Soc. London, Ser. A **179**, 69 (1941).

[15]S. Pei, N. J. Zaluzec, J. D. Jorgensen, B. Dabrowski, D. G. Hinks, A. W. Mitchell, and D. R. Ricahrds, Phys. Rev. B **39**, 811 (1989).

[16]S. Pei, J. D. Jorgensen, B. Dabrowski, D. G. Hinks, D. R. Richards, A. W. Mitchell, J. M. Newsam, S. K. Sinha, D. Vaknin, and A. J. Jacobson, Phys. Rev. B **41**, 4126 (1990).

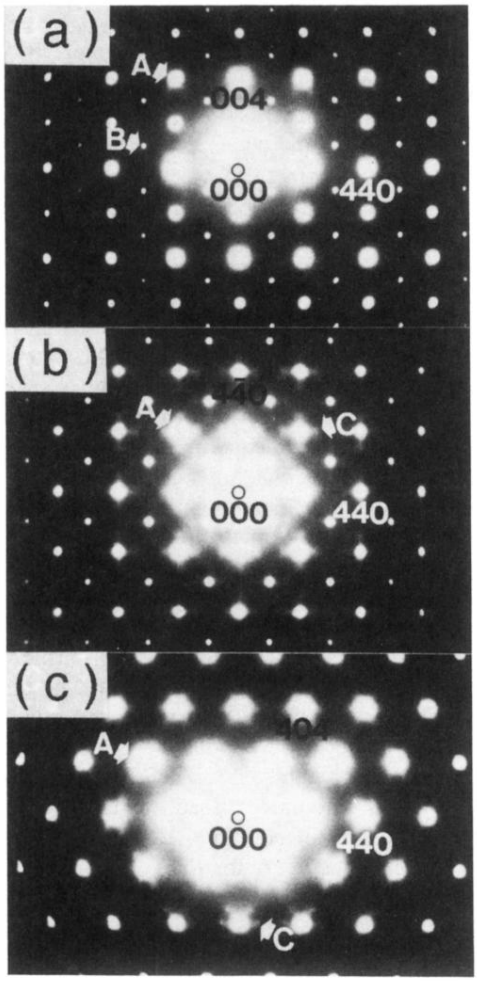

FIG. 1. Electron-diffraction patterns of Ba-Pb-Bi-O with $x = 0.25$ taken at room temperature. Electron incidences for (a), (b), and (c) are, respectively, parallel to the $[1\bar{1}0]$, $[00\bar{1}]$, and $[1\bar{1}\,\bar{1}]$ directions.

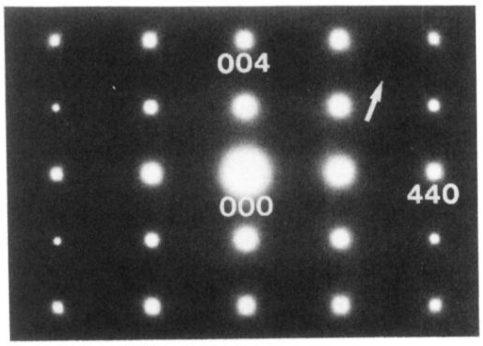

FIG. 10. Electron-diffraction pattern taken at 543 K for $x = 0.25$. The electron incidence is parallel to the $[1\bar{1}0]$ direction.

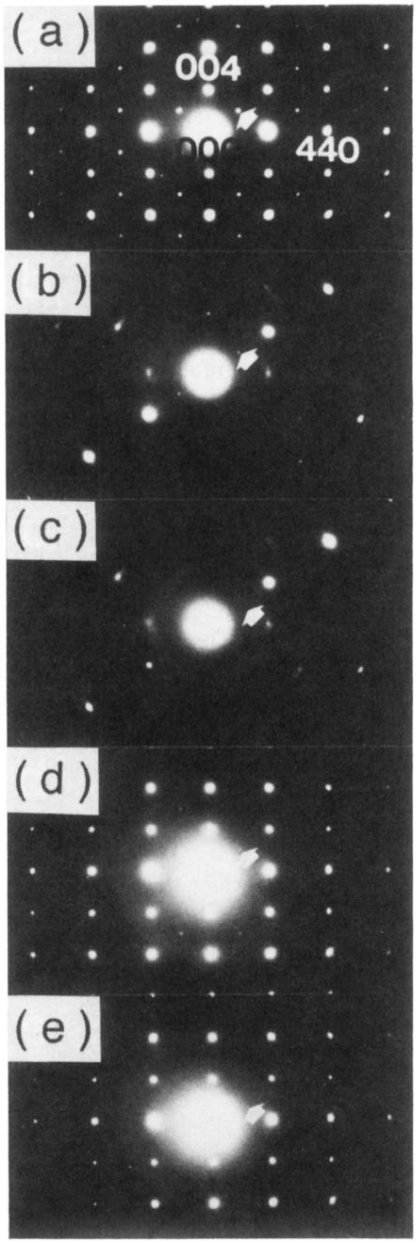

FIG. 12. Electron-diffraction patterns of Ba-Pb-Bi-O with $x=0.50$ at various temperatures during the heating process. The pattern were taken at room temperature for (a) and (b), at 470 K for (c) and (d), and at 600 K for (e). Electron incidences for (a), (d), and (e) are parallel to the $[1\bar{1}0]$ direction, although the patterns for (b) and (c) were taken by rotating the specimen about the [111] direction in order to obtain the double-diffraction free condition. Because the 111 superlattice spot indicated by the arrow vanishes in (c), the spot observed in (d) is due to the double diffraction.

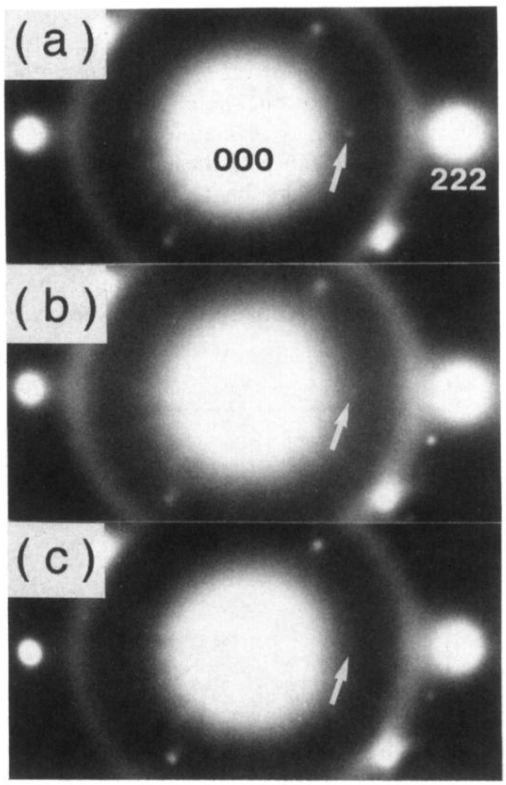

FIG. 13. Electron-diffraction patterns showing a change in the intensity of thermal diffuse scattering in the tetragonal phase taken at (a) 297 K, (b) 393 K, and (c) 468 K, respectively. The specimen is slightly rotated in order to avoid the double diffraction. A halo pattern observed is due to a carbon film used for coating a copper grid.

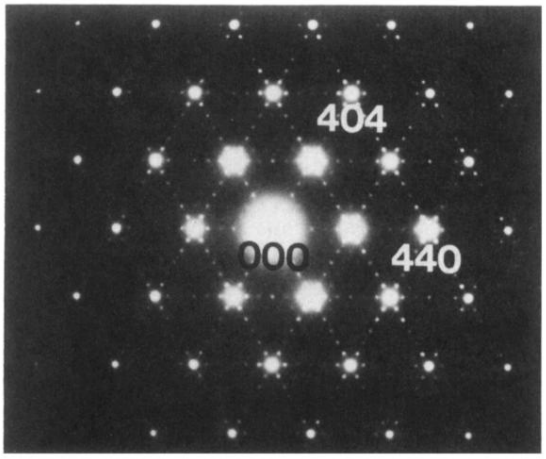

FIG. 15. Electron-diffraction pattern of Ba-Pb-Bi-O with $x = 1.00$ taken at about 400 K. The electron incidence is parallel to the $[1\bar{1}\,\bar{1}]$ direction.

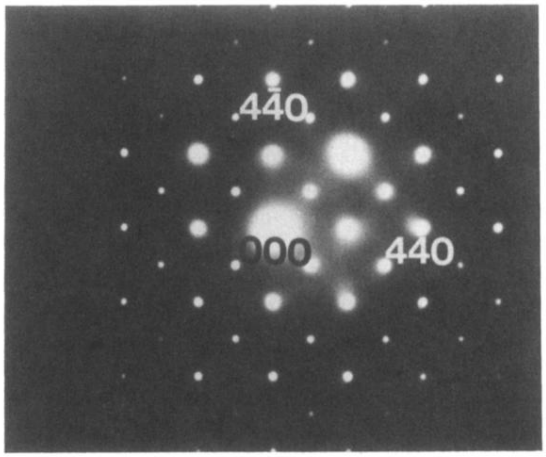

FIG. 16. Electron-diffraction pattern of Ba-Pb-Bi-O with $x = 1.00$ taken at about 110 K.

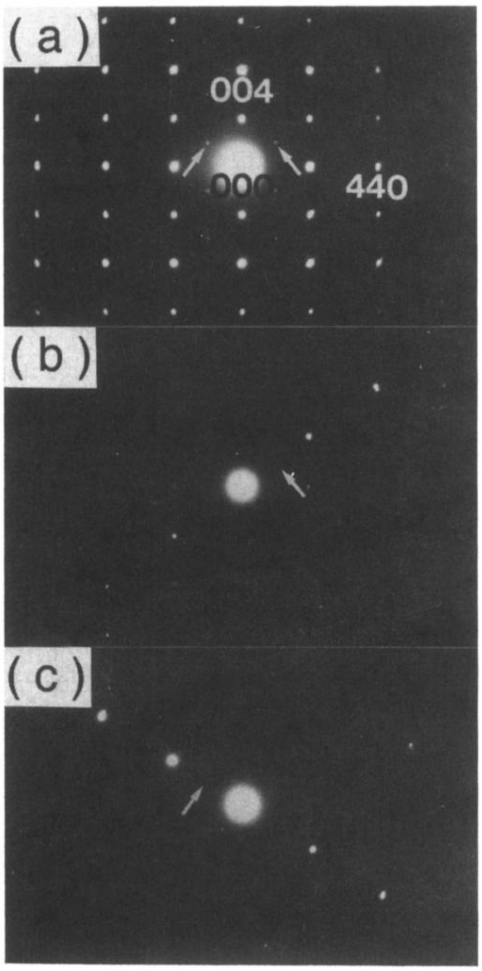

FIG. 2. Electron-diffraction patterns of Ba-Pb-Bi-O with $x=0.25$. The electron incidence for (a) is parallel to the $[1\bar{1}0]$ direction. The patterns of (b) and (c) were taken by rotating the specimen about the [111] and $[11\bar{1}]$ directions, respectively. The 111 and $\bar{1}\,\bar{1}1$ superlattice spots indicated by the arrows in (a) vanish in (b) and (c).

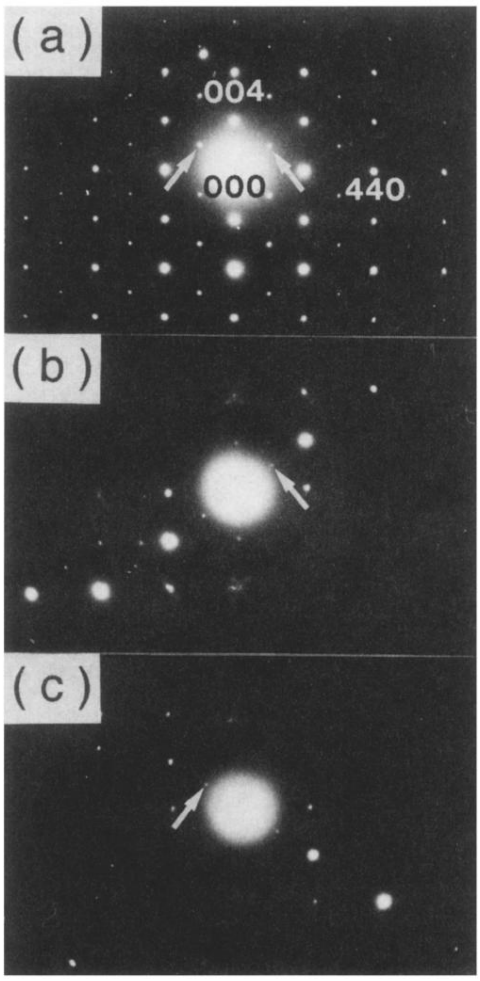

FIG. 4. Electron-diffraction patterns of Ba-Pb-Bi-O with $x = 0.50$ taken at room temperature. The condition for taking the patterns of (a), (b), and (c) are the same as in the case of $x = 0.25$. The 111 and $\bar{1}\bar{1}1$ spots indicated by the arrows are found in (a), (b), and (c).

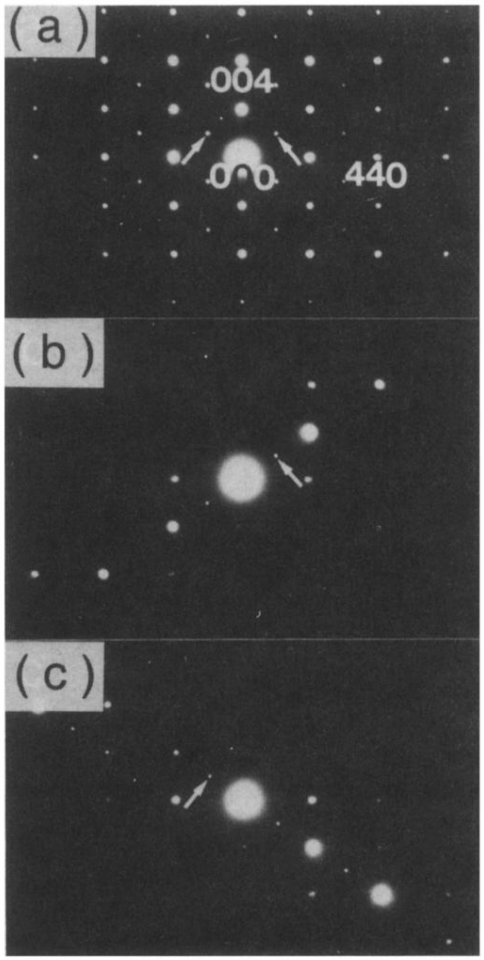

FIG. 6. Electron-diffraction patterns of Ba-Pb-Bi-O with $x = 1.00$ taken at room temperature. The condition for taking the patterns of (a), (b), and (c) are the same as in $x = 0.25$ and 0.50. The 111 and $\bar{1}\,\bar{1}1$ spots indicated by arrows appear in (a), (b), and (c), just as in $x = 0.50$.

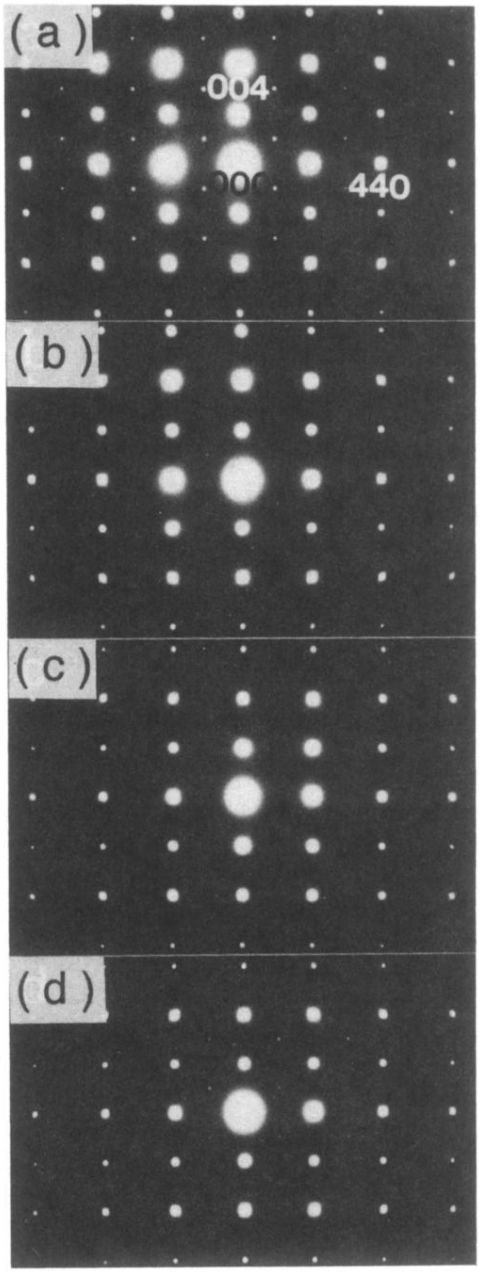

FIG. 8. Electron-diffraction patterns of Ba-Pb-Bi-O with $x=0.25$ at various temperatures during the process of heating and subsequent cooling. Electron incidences for all patterns are parallel to the $[1\bar{1}0]$ direction. The patterns were, respectively, taken at (a) room temperature, (b) 450 K, (c) 540 K, and (d) room temperature.